Paper C

Exact Volume Balance Versus Exact Mass Balance in Compositional Reservoir Simulation *

* Submitted to *Computational Geosciences*, December 2005.

Exact Volume Balance Versus Exact Mass Balance in Compositional Reservoir Simulation

Jarle Haukås (jarle.haukas@cipr.uib.no), Ivar Aavatsmark and Magne Espedal
Centre for Integrated Petroleum Research (CIPR), University of Bergen, Norway

Edel Reiso
Norsk Hydro Oil & Energy Research Centre, Bergen, Norway

Abstract. A new compositional formulation which incorporates both an exact volume balance approach and an exact mass balance approach has been developed and tested. The formulation is based on combining the conventional mass balance requirement with volume/isochoric balance requirements. The primary variables are pressure, saturations and isochoric variables, and both a fully implicit version and an IMPSAT version (implicit in pressure and saturations, explicit in the isochoric variables) are included. We note that the formulation reduces to a fully implicit black-oil formulation when used with saturated black-oil fluid properties.

A comparison to similar approaches is provided, and the performance of the exact volume balance approach versus that of the exact mass balance approach is investigated. Our conclusions are in favour of the exact volume balance approach. Numerical results are shown.

Keywords: compositional, mass balance, volume balance, isochoric variables, fully implicit, IMPSAT, comparison

1. Introduction

A compositional model usually involves of a set of mass balance equations, volume balance constraints and phase equilibrium equations. The thermodynamic relations are most often based on an equation of state. For an isothermal model, the number of primary variables and equations equals the number of (pseudo) components in the system.

In a black-oil model, the hydrocarbon phases are assumed to consist of only two (pseudo) components. This assumption simplifies the phase equilibrium computations, but in cases with large compositional gradients, the black-oil fluid description is not sufficiently precise.

Traditionally, black-oil and compositional simulation has been performed with different simulators. The reason for this is that the conventional compositional formulation uses pressure and component mole numbers (or pressure, overall composition and overall density) as primary variables, e.g., [1], while the conventional black-oil formulation uses pressure and saturations as primary variables.

Fluid flow is governed by Darcy's law, which is basically a relation in pressure and saturations. In addition, the requirement that the fluids must fill the pore volume is naturally given in terms of saturations. Pressure and saturations are therefore convenient primary variables.

A compositional formulation which includes pressure and saturations among the primary variables will reduce to the conventional black-oil formulation when used with saturated black-oil fluid properties. Having a unified black-oil and compositional formulation leads to reduced simulator development and maintenance costs. Several such formulations have been proposed in the literature, e.g., [2–7].

Furthermore, the pressure and saturations part can be decoupled from the rest of the system, by combining the mass balance equations into pressure and saturation equations, and using an IMPSAT approach (interblock flow terms implicit in pressure and saturations only). Consequently, the black-oil part of the compositional system is identified. Different IMPSAT approaches have also been proposed, e.g., [4, 6, 7].

The combination of mass balance equations has been discussed by several authors. Young and Stephenson, [1], Coats, [2], Coats et al., [5] and Cao, [6], use Gaussian elimination of the Jacobian of the linearized system. The volume balance method of Watts, [3], originally proposed by Ács et al., [8], bases the derivation on physical principles.

Wong et al., [9], showed that Gaussian elimination and the volume balance method yield the same system of finite-difference equations at the start of a timestep. Coats, [10], commented that the pressure equation is unique, independent of the manner of derivation.

However, for the mentioned formulations, two different approaches are used. Some formulations, e.g., [2, 6], involve a mass balance residual, but yield exact volume balance. Others, e.g., [1, 3, 5, 8], involve a volume balance residual, but yield exact mass balance. Coats et al., [5], report that the use of a relaxed volume balance instead of a mass balance residual leads to better convergence properties. Unfortunately, no numerical evidence has been given to support that statement.

This paper aims at clarifying the distinction between exact volume balance and exact mass balance. Motivated by the ideas of the volume balance method and the ideas of isochoric variables and equations introduced by Haukås et al., [7], we replace the conventional linearized mass balance scheme by a volume/isochoric balance scheme which still takes the mass balance into account. The scheme can be used for either exact volume balance or exact mass balance. The primary variables are pressure, saturations and isochoric variables, and both a fully implicit version and an IMPSAT version are included. The formulation is compared to similar approaches, and the performance of exact volume balance versus exact mass balance is investigated.

2. Background

In the following, we consider the N_c mass balance equations, and their combination into physically interpretable, weighted sums (e.g., volume balance equations, [3]). Here, N_c is the number of components. The starting point is the integral form

$$\int_{V_b} \frac{\partial}{\partial t}\left(\phi \frac{\boldsymbol{n}}{V_T}\right) dV + \int_{S_b} \hat{\boldsymbol{f}} \cdot \vec{n}\, dS - \int_{V_b} \hat{\boldsymbol{q}}\, dV = \boldsymbol{0}, \tag{1}$$

where ϕ is the porosity, $\boldsymbol{n}$ is the N_c vector of component amounts, V_T is the total fluid volume, $\hat{\boldsymbol{f}}$ contains the N_c component fluxes, $\hat{\boldsymbol{q}}$ is the N_c vector of source density rates, while V_b is some (bulk) volume with surface S_b. The unit normal of S_b is denoted $\vec{n}$. We note that each component flux in $\hat{\boldsymbol{f}}$ is a vector in space. The dot product in (1) is taken for each component flux, so that $\hat{\boldsymbol{f}} \cdot \vec{n}$ is a N_c vector.

We observe that (1) is given in terms of both extensive and intensive quantities. Extensive quantities, for instance volumes and mole numbers, depend on the amount of material present, while intensive quantities, for instance porosity and densities, do not. To describe the intensive properties of an isothermal system, N_c independent intensive parameters are needed. If extensive properties are to be determined, $N_c + 1$ parameters are needed, of which at least one must be extensive.

We first show how the differential form of the equations can be weighted and combined, and then consider the control-volume finite-difference forms. For the latter, the concepts of mass balance, volume balance and isochoric balance are defined, and it is shown that the weighting procedure is not straight-forward.

2.1. Differential form

The differential form of (1) is based on an assumption of continuity, and must be given in terms of intensive quantities only. This leads to

$$\frac{\partial}{\partial t}\left(\phi \frac{\boldsymbol{z}}{v_T}\right) + \nabla \cdot \hat{\boldsymbol{f}} - \hat{\boldsymbol{q}} = \boldsymbol{0}, \tag{2}$$

where $\boldsymbol{z} = (1/n_T)\,\boldsymbol{n}$ is the overall composition, $v_T = V_T/n_T$ is the total specific volume and n_T is the total mass (sum over all components). We note that the divergence is taken for each component flux in $\hat{\boldsymbol{f}}$.

Watts, [3], showed that a weighting of (2) by the total partial molar volumes $(\partial V_T/\partial \boldsymbol{n})_p$ yields a pressure equation of the form

$$\frac{\partial \phi}{\partial t} - \frac{\phi}{v_T}\left(\frac{\partial v_T}{\partial p}\right)_{\boldsymbol{z}} \frac{\partial p}{\partial t} + \left(\frac{\partial V_T}{\partial \boldsymbol{n}}\right)_p \left(\nabla \cdot \hat{\boldsymbol{f}} - \hat{\boldsymbol{q}}\right) = 0, \tag{3}$$

while a weighting by the partial volumes of phase j, $\left(\partial V^j/\partial \boldsymbol{n}\right)_p$, yields a saturation equation of the form

$$\frac{\partial}{\partial t}\left(\phi S^j\right) - \frac{\phi}{v_{\mathrm{T}}}\left(\frac{\partial v^j}{\partial p}\right)_{\boldsymbol{z}} \frac{\partial p}{\partial t} + \left(\frac{\partial V^j}{\partial \boldsymbol{n}}\right)_p \left(\nabla \cdot \hat{\boldsymbol{f}} - \hat{\boldsymbol{q}}\right) = 0. \tag{4}$$

Here, p is pressure, S^j is the saturation of phase j, V^j is the phase volume and $v^j = V^j/n_{\mathrm{T}}$ is the phase specific volume.

We note that derivatives of extensive variables with respect to extensive variables are intensive quantities. Consequently, (3) and (4) are given in terms of intensive quantities only, as required.

Equation (3) can be interpreted as the differential version of the requirement that the fluids must fill the pore space, i.e., $V_{\mathrm{T}} = V_{\mathrm{p}}$, where V_{p} denotes the pore volume. Similarly, equation (4) can be interpreted as the differential version of $V^j = V_{\mathrm{p}} S^j$. In other words, (3) and (4) are volume balance equations. Since the saturations are supposed to sum to unity, and the phase volumes sum to the total volume, a sum of (4) over all phases yields the pressure equation (3). Consequently, the volume balance equations constitute N_{p} independent equations, where N_{p} is the number of phases.

If used in practice, the volume balance equations replace N_{p} of the mass balance equations. Since it is not clear which mass balance equations should be replaced, $N_{\mathrm{c}} - N_{\mathrm{p}}$ additional equations replacing the rest of the mass balance equations should also be introduced. If these equations are complementary to the volume balance equations, the properties of the original system are preserved. This corresponds to the idea of isochoric equations introduced by Haukås et al., [7].

However, Haukås et al. did not consider the differential form of the equations. Furthermore, the differential form is seldom used for real problems, as the flow terms $\hat{\boldsymbol{f}}$ depend on a discontinuous permeability field. The integral form of the equations is therefore required.

2.2. Integral (control-volume discretized) form

For the solution of (1), a control-volume discretization is convenient. The bulk volume V_{b} is assumed to be a known, time-independent parameter, and the properties within V_{b} are assumed to be constant over that volume. This allows for the form

$$\frac{\partial}{\partial t}\left(\phi \frac{\boldsymbol{n}}{V_{\mathrm{T}}} V_{\mathrm{b}}\right) + \boldsymbol{f} - \boldsymbol{q} = \boldsymbol{0}, \tag{5}$$

where $\boldsymbol{f}$ is the N_{c} vector of discretized component flow rates, while $\boldsymbol{q}$ is the N_{c} vector of component source rates. In addition, we use the total

volume balance requirement, $V_{\mathrm{T}} = V_{\mathrm{p}} = \phi V_{\mathrm{b}}$, to obtain

$$\frac{\partial \boldsymbol{n}}{\partial t} + \boldsymbol{\theta} = \mathbf{0}, \tag{6}$$

where

$$\boldsymbol{\theta} = \boldsymbol{f} - \boldsymbol{q} \tag{7}$$

is introduced for notational convenience.

Before considering a weighting of (6), we present some possible conservation requirements.

2.2.1. *Mass balance*
Conventionally, the time derivative in (6) is approximated by a backward difference, leading to the form

$$\Delta \boldsymbol{n} + \boldsymbol{\theta} \Delta t = \mathbf{0}, \tag{8}$$

where

$$\Delta t = t^n - t^{n-1}, \qquad \Delta \boldsymbol{n} = \boldsymbol{n}^n - \boldsymbol{n}^{n-1}. \tag{9}$$

The form (8) applies to each control volume, and common flow terms are used for flow through a common surface of two control-volumes. This ensures local mass balance. Furthermore, the sum of (8) over all control-volumes expresses a global mass balance, i.e., that the net change of mass equals the net mass introduced into the system. Note that, for generality, we do not specify the timelevel at which $\boldsymbol{\theta}$ is evaluated, i.e., $\boldsymbol{\theta}$ can be either fully implicit or partly explicit in time.

2.2.2. *Volume balance*
The requirement that the fluids must fill the pore space is important. We let the N_{p} vector $\boldsymbol{V}$ represent the fluid volumes, and let the N_{p} vector $\boldsymbol{V}_{\mathrm{p}}$ represent the corresponding parts of the pore volume. Examples of representations of $\boldsymbol{V}$ and $\boldsymbol{V}_{\mathrm{p}}$ for a three-phase system are

$$\boldsymbol{V} = \begin{bmatrix} V^o \\ V^g \\ V^w \end{bmatrix}, \qquad \boldsymbol{V}_{\mathrm{p}} = \phi V_{\mathrm{b}} \begin{bmatrix} S^o \\ S^g \\ S^w \end{bmatrix}, \qquad S^o + S^g + S^w = 1, \tag{10}$$

and

$$\boldsymbol{V} = \begin{bmatrix} V_{\mathrm{T}} \\ V^g \\ V^w \end{bmatrix}, \qquad \boldsymbol{V}_{\mathrm{p}} = \phi V_{\mathrm{b}} \begin{bmatrix} 1 \\ S^g \\ S^w \end{bmatrix}, \qquad S^o + S^g + S^w = 1. \tag{11}$$

Here, superscripts o, g and w denote the oil, gas and water phases, respectively. In the latter representation, S^g and S^w have been chosen to be primary saturations. Other choices are of course possible.

Based on this notation, we introduce the general volume balance requirement

$$\boldsymbol{V}_{\mathrm{p}} - \boldsymbol{V} = \boldsymbol{0}, \qquad S^o + S^g + S^w = 1. \tag{12}$$

2.2.3. *Isochoric balance*
As a supplement to the volume balance requirement (12), we propose an isochoric balance requirement,

$$\boldsymbol{x}_{\mathrm{p}} - \boldsymbol{W}_x \, \boldsymbol{n} = \boldsymbol{0}, \tag{13}$$

where the $N_{\mathrm{c}} - N_{\mathrm{p}}$ vector $\boldsymbol{x}_{\mathrm{p}}$ is referred to as the isochoric variables, while the rows of the $(N_{\mathrm{c}} - N_{\mathrm{p}}) \times N_{\mathrm{c}}$ matrix $\boldsymbol{W}_x$ span the nullspace of the $N_{\mathrm{p}} \times N_{\mathrm{c}}$ matrix $\boldsymbol{W}_V = (\partial \boldsymbol{V} / \partial \boldsymbol{n})_p$ of partial volumes. During a timestep, $\boldsymbol{W}_x$ is kept fixed, usually the previous time level.

The motivation for (13) is due to Haukås et al., [7]. As

$$\boldsymbol{V} = \left(\frac{\partial \boldsymbol{V}}{\partial \boldsymbol{n}} \right)_p \boldsymbol{n} = \boldsymbol{W}_V \, \boldsymbol{n}, \tag{14}$$

and $\boldsymbol{W}_x$ spans the nullspace of $\boldsymbol{W}_V$, which is the orthogonal complement of the row space of $\boldsymbol{W}_V$, the isochoric variables are complementary to volumes. Consequently, information provided by the mole numbers $\boldsymbol{n}$ is preserved by the alternative set $(\boldsymbol{V}, \boldsymbol{x}_{\mathrm{p}})$.

We now turn to the weighting of the mass balance equations (6). By differentiating through $V_{\mathrm{T}} = \phi V_{\mathrm{b}}$, assuming that $V_{\mathrm{T}} = V_{\mathrm{T}}(p, \boldsymbol{n})$, we find that

$$V_{\mathrm{b}} \frac{\partial \phi}{\partial t} = \frac{\partial V_{\mathrm{T}}}{\partial t} = \left(\frac{\partial V_{\mathrm{T}}}{\partial p} \right)_{\boldsymbol{n}} \frac{\partial p}{\partial t} + \left(\frac{\partial V_{\mathrm{T}}}{\partial \boldsymbol{n}} \right) \frac{\partial \boldsymbol{n}}{\partial t}. \tag{15}$$

Consequently, if we multiply (6) by $(\partial V_{\mathrm{T}} / \partial \boldsymbol{n})_p$, and use (15), we obtain

$$V_{\mathrm{b}} \frac{\partial \phi}{\partial t} - \left(\frac{\partial V_{\mathrm{T}}}{\partial p} \right)_{\boldsymbol{n}} \frac{\partial p}{\partial t} + \left(\frac{\partial V_{\mathrm{T}}}{\partial \boldsymbol{n}} \right)_p \boldsymbol{\theta} = 0, \tag{16}$$

which is similar to (3). Furthermore, by differentiating through $V^j = \phi V_{\mathrm{b}} S^j$ with the assumption that $V^j = V^j(p, \boldsymbol{n})$, we find that

$$V_{\mathrm{b}} \frac{\partial}{\partial t} \left(\phi S^j \right) = \frac{\partial V^j}{\partial t} = \left(\frac{\partial V^j}{\partial p} \right)_{\boldsymbol{n}} \frac{\partial p}{\partial t} + \left(\frac{\partial V^j}{\partial \boldsymbol{n}} \right)_p \frac{\partial \boldsymbol{n}}{\partial t}. \tag{17}$$

If we multiply (6) by $(\partial V^j / \partial \boldsymbol{n})_p$, and use (17), we obtain

$$V_{\mathrm{b}} \frac{\partial}{\partial t} \left(\phi S^j \right) - \left(\frac{\partial V^j}{\partial p} \right)_{\boldsymbol{n}} \frac{\partial p}{\partial t} + \left(\frac{\partial V^j}{\partial \boldsymbol{n}} \right)_p \boldsymbol{\theta} = 0, \tag{18}$$

which is similar to (4). By introducing $\boldsymbol{V}_\mathrm{p}$ and $\boldsymbol{V}$, we may represent (16) and (18) by the N_p independent equations

$$\frac{\partial \boldsymbol{V}_\mathrm{p}}{\partial t} - \left(\frac{\partial \boldsymbol{V}}{\partial p}\right)_{\boldsymbol{n}} \frac{\partial p}{\partial t} + \left(\frac{\partial \boldsymbol{V}}{\partial \boldsymbol{n}}\right)_{p} \boldsymbol{\theta} = \mathbf{0}. \tag{19}$$

In addition, motivated by Haukås et al., [7], we multiply (6) by the time-independent $(N_\mathrm{c} - N_\mathrm{p}) \times N_\mathrm{c}$ matrix $\boldsymbol{W}_x$ to obtain

$$\frac{\partial \boldsymbol{x}_\mathrm{p}}{\partial t} + \boldsymbol{W}_x \boldsymbol{\theta} = \mathbf{0}. \tag{20}$$

We approximate the time derivatives in (19) and (20) by backward differences, leading to

$$\Delta \boldsymbol{V}_\mathrm{p} - \left(\frac{\partial \boldsymbol{V}}{\partial p}\right)_{\boldsymbol{n}} \Delta p + \left(\frac{\partial \boldsymbol{V}}{\partial \boldsymbol{n}}\right)_{p} \boldsymbol{\theta} \Delta t = \mathbf{0}, \tag{21}$$

$$\Delta \boldsymbol{x}_\mathrm{p} + \boldsymbol{W}_x \boldsymbol{\theta} \Delta t = \mathbf{0}. \tag{22}$$

However, (21) and (22) are not consistent with the conventional mass balance (8), but rather with

$$\frac{\partial \boldsymbol{n}}{\partial p} \Delta p + \frac{\partial \boldsymbol{n}}{\partial \boldsymbol{S}_\mathrm{p}} \Delta \boldsymbol{S}_\mathrm{p} + \frac{\partial \boldsymbol{n}}{\partial \boldsymbol{x}_\mathrm{p}} \Delta \boldsymbol{x}_\mathrm{p} + \boldsymbol{\theta} \Delta t = \mathbf{0}, \tag{23}$$

where $\boldsymbol{S}_\mathrm{p}$ contains $N_\mathrm{p} - 1$ primary saturations, see appendix A.

If we solve (23) instead of (8), the conventional mass balance is obtained only when $\Delta t \to 0$. This inconsistency arises from expressing time derivatives of mass in terms of time derivatives of other variables, as for instance is done in Watts' derivation of the differential form of the volume balance equations, [3]. Such an approach only preserves the original mass balance in the continuous (differential) case.

Watts does not address this problem directly. However, for the purpose of interpretation, he uses $V_\mathrm{T} = \phi V_\mathrm{b}$ to derive the form

$$\left[V_\mathrm{b} \frac{\partial \phi}{\partial p} - \left(\frac{\partial V_\mathrm{T}}{\partial p}\right)_{\boldsymbol{n}}\right]^{n-1} \Delta p + \left(\frac{\partial V_\mathrm{T}}{\partial \boldsymbol{n}}\right)_{p}^{n-1} \boldsymbol{\theta} \Delta t = \left(V_\mathrm{T} - V_\mathrm{p}\right)^{n-1}, \tag{24}$$

which is similar to (16), except for the term on the right hand side. Furthermore, Watts reports that he uses a solution of the pressure and saturation equations to determine $\boldsymbol{\theta}$, followed by

$$\boldsymbol{n}^n = \boldsymbol{n}^{n-1} - \boldsymbol{\theta} \Delta t. \tag{25}$$

Subsequent to (25), Watts uses a phase equilibrium calculation with $(p, \boldsymbol{n})$ to recalculate the fluid volumes, so that $(V^j - V_\mathrm{p} S^j)$ and thereby

$(V_{\mathrm{T}} - V_{\mathrm{p}})$ become non-zero. The latter is taken into account by (24), and Watts states that the phase volume discrepancies can be resolved in much the same way. Consequently, Watts overcomes the mass balance inconsistency, and actually obtains an exact mass balance, (25).

Watts' approach is a possible solution to the mass balance inconsistency problem, but it requires that the flow rates and source terms are determined as functions of pressure and saturations only. Otherwise, additional equations, e.g., isochoric equations, are needed. Furthermore, the use of an iterative scheme would increase control of the volume discrepancies. The latter corresponds to replacing the timestep superscripts of (24) by iteration step superscripts, and is also suggested by Wong et al., [9].

However, due to the right hand side of (24), Watts' approach does not correspond to a weighting of the mass balance equations. Actually, a weighting of the mass balance equations is of no interest if the residuals of those equations are zero. In order to obtain an alternative, weighted mass balance approach, we should exclude the direct update (25) and the volume discrepancies $(V^j - V_{\mathrm{p}}S^j)$, but include a (weighted) mass balance discrepancy.

3. New Principles

In the following, we propose a formulation which incorporates an approach similar to that of Watts, but including isochoric equations, and an approach without volume discrepancies. The former yields exact mass balance, while the latter yields exact volume balance, and is a weighted mass balance approach.

In order to clarify the distinction between exact mass balance and exact volume balance, we seek a common form of the iterative scheme. Rather than using a weighting of the mass balance equations as a starting point, we consider a combination of the linearized mass balance requirement (8) and the linearized volume/isochoric balance requirements (12) and (13), where we make sure that the partial volumes appear. Consequently, in the case of no volume/isochoric discrepancies, the scheme actually reduces to a weighted mass balance scheme.

The linearization is with respect to the primary variables. However, due to the thermodynamic relations, which cannot be written explicitly in terms of the primary variables, a set of secondary variables is also required. For each secondary variable we need a secondary equation, and the secondary equations will be fulfilled at every iteration level. As will become clear, the choice of secondary equations is a choice between exact volume balance and exact mass balance.

3.1. Primary and secondary variables

As mentioned in section 2, we need $N_c + 1$ independent parameters, including an extensive one, to determine all intensive and extensive properties of the system. We use the set $(p, \boldsymbol{S}_p, \boldsymbol{x}_p, V_b)$, where $\boldsymbol{S}_p$ contains $N_p - 1$ primary saturations, and $\boldsymbol{x}_p$ denotes the $N_c - N_p$ isochoric variables, defined by (13). Omitting one saturation ensures that the saturations sum to unity, as required by (12). We treat V_b as a known parameter, and let $\boldsymbol{u}_p = (p, \boldsymbol{S}_p, \boldsymbol{x}_p)$ be the set of N_c primary variables.

The thermodynamic properties of the phases are conventionally given in terms of pressure and the component mole numbers of the phases, denoted $\boldsymbol{n^j}$. We assume that water and hydrocarbons do not interact, i.e., that water does not exist in the hydrocarbon phases, and that hydrocarbons may not dissolve in the water phase. This means that there are $N_s = N_{hp}N_{hc} + N_{wc} = (N_{hp} - 1)\, N_{hc} + N_c$ phase mole numbers. Here, N_{hp} is the number of hydrocarbon phases (zero, one or two), N_{hc} is the number of hydrocarbon components, while N_{wc} is the number of water components (zero or one). The phase mole numbers form a convenient set of N_s secondary variables, $\boldsymbol{u}_s = \boldsymbol{n^j}$.

3.2. Primary and secondary equations

In addition to the $2N_c$ conservation requirements (8), (12) and (13), we impose chemical equilibrium between the hydrocarbon phases,

$$\boldsymbol{f}^o - \boldsymbol{f}^g = \boldsymbol{0}, \tag{26}$$

where $\boldsymbol{f}^o$ and $\boldsymbol{f}^g$ are N_{hc} vectors containing the component fugacities of the oil and gas phases, respectively. The fugacity equalities (26) are very important. Actually, at any level where we want to calculate the volume derivatives $(\partial \boldsymbol{V}/\partial p)_{\boldsymbol{n}}$ and $(\partial \boldsymbol{V}/\partial \boldsymbol{n})_p$, the phase equilibrium requirement (26) must be fulfilled, see appendix B.1.

If there is only one hydrocarbon phase, (26) is redundant. Consequently, (26) constitutes $(N_{hp} - 1)\, N_{hc}$ equations. Together with the conservation requirements, we have $2N_c + (N_{hp} - 1)\, N_{hc}$ equations, which is the same as the number of primary and secondary variables.

The iterative scheme for determining the primary variables must include N_c equation residuals. The remaining $N_c + (N_{hp} - 1)\, N_{hc}$ equations are used to determine the secondary variables, and will be fulfilled at every iteration step. To be able to calculate precise volume derivatives, the fugacity equalities (26) must be included among the secondary equations. The N_c additional secondary equations will be either the mass balance requirement (8) or the volume/isochoric balance requirements (12) and (13).

3.3. Iterative scheme

In order to form a common iterative scheme, we consider residuals of all of the conservation requirements, even though N_c of them will be fulfilled at every iteration level. The derivation is based on a linearization of the conservation requirements with respect to $\boldsymbol{u}_\mathrm{p}$. We omit subscripts on derivatives with respect to these variables, assuming that they represent total derivatives, see appendix B.2.

A linearization of the mass balance equations (8) yields

$$\begin{aligned}
&\left(\frac{\partial \boldsymbol{n}}{\partial p}\right)^{(k)} \Delta p^{(k+1)} + \left(\frac{\partial \boldsymbol{n}}{\partial \boldsymbol{S}_\mathrm{p}}\right)^{(k)} \Delta \boldsymbol{S}_\mathrm{p}^{(k+1)} + \left(\frac{\partial \boldsymbol{n}}{\partial \boldsymbol{x}_\mathrm{p}}\right)^{(k)} \Delta \boldsymbol{x}_\mathrm{p}^{(k+1)} \\
+ &\left(\frac{\partial \boldsymbol{\theta}}{\partial \boldsymbol{u}_\mathrm{p}}\right)^{(k)} \Delta t\, \Delta \boldsymbol{u}_\mathrm{p}^{(k+1)} \\
= &-\left(\Delta \boldsymbol{n} + \boldsymbol{\theta} \Delta t\right)^{(k)}. \qquad (27)
\end{aligned}$$

Furthermore, assuming that $\boldsymbol{V} = \boldsymbol{V}\left(p, \boldsymbol{n}\right)$, we find that

$$\frac{\partial \boldsymbol{V}}{\partial u} = \left(\frac{\partial \boldsymbol{V}}{\partial p}\right)_{\boldsymbol{n}} \frac{\partial p}{\partial u} + \left(\frac{\partial \boldsymbol{V}}{\partial \boldsymbol{n}}\right)_{p} \frac{\partial \boldsymbol{n}}{\partial u}, \qquad (28)$$

for any $u \in (p, \boldsymbol{S}_\mathrm{p}, \boldsymbol{x}_\mathrm{p})$. We also assume that $\boldsymbol{V}_\mathrm{p} = \boldsymbol{V}_\mathrm{p}\left(p, \boldsymbol{S}_\mathrm{p}\right)$. Consequently, a linearization of the volume balance requirement (12) yields

$$\begin{aligned}
&\left[\left(\frac{\partial \boldsymbol{V}_\mathrm{p}}{\partial p}\right)^{(k)} - \left(\frac{\partial \boldsymbol{V}}{\partial p}\right)_{\boldsymbol{n}}^{(k)}\right] \Delta p^{(k+1)} + \left(\frac{\partial \boldsymbol{V}_\mathrm{p}}{\partial \boldsymbol{S}_\mathrm{p}}\right)^{(k)} \Delta \boldsymbol{S}_\mathrm{p}^{(k+1)} \\
- &\left(\frac{\partial \boldsymbol{V}}{\partial \boldsymbol{n}}\right)_{p}^{(k)} \left(\frac{\partial \boldsymbol{n}}{\partial p}\right)^{(k)} \Delta p^{(k+1)} - \left(\frac{\partial \boldsymbol{V}}{\partial \boldsymbol{n}}\right)_{p}^{(k)} \left(\frac{\partial \boldsymbol{n}}{\partial \boldsymbol{S}_\mathrm{p}}\right)^{(k)} \Delta \boldsymbol{S}_\mathrm{p}^{(k+1)} \\
- &\left(\frac{\partial \boldsymbol{V}}{\partial \boldsymbol{n}}\right)_{p}^{(k)} \left(\frac{\partial \boldsymbol{n}}{\partial \boldsymbol{x}_\mathrm{p}}\right)^{(k)} \Delta \boldsymbol{x}_\mathrm{p}^{(k+1)} \\
= &-\left(\boldsymbol{V}_\mathrm{p} - \boldsymbol{V}\right)^{(k)}. \qquad (29)
\end{aligned}$$

With the use of (27), we arrive at the form

$$\begin{aligned}
&\left[\left(\frac{\partial \boldsymbol{V}_\mathrm{p}}{\partial p}\right)^{(k)} - \left(\frac{\partial \boldsymbol{V}}{\partial p}\right)_{\boldsymbol{n}}^{(k)}\right] \Delta p^{(k+1)} + \left(\frac{\partial \boldsymbol{V}_\mathrm{p}}{\partial \boldsymbol{S}_\mathrm{p}}\right)^{(k)} \Delta \boldsymbol{S}_\mathrm{p}^{(k+1)} \\
+ &\left(\frac{\partial \boldsymbol{V}}{\partial \boldsymbol{n}}\right)_{p}^{(k)} \left(\frac{\partial \boldsymbol{\theta}}{\partial \boldsymbol{u}_\mathrm{p}}\right)^{(k)} \Delta t\, \Delta \boldsymbol{u}_\mathrm{p}^{(k+1)} \\
= &-\left(\boldsymbol{V}_\mathrm{p} - \boldsymbol{V}\right)^{(k)} - \left(\frac{\partial \boldsymbol{V}}{\partial \boldsymbol{n}}\right)_{p}^{(k)} \left(\Delta \boldsymbol{n} + \boldsymbol{\theta} \Delta t\right)^{(k)}. \qquad (30)
\end{aligned}$$

In addition, a linearization of the isochoric balance (13),

$$\begin{aligned}
&\Delta \boldsymbol{x}_{\mathrm{p}}^{(k+1)} - \boldsymbol{W}_x \left(\frac{\partial \boldsymbol{n}}{\partial p}\right)^{(k)} \Delta p^{(k+1)} \\
-\ &\boldsymbol{W}_x \left[\left(\frac{\partial \boldsymbol{n}}{\partial \boldsymbol{S}_{\mathrm{p}}}\right)^{(k)} \Delta \boldsymbol{S}_{\mathrm{p}}^{(k+1)} + \left(\frac{\partial \boldsymbol{n}}{\partial \boldsymbol{x}_{\mathrm{p}}}\right)^{(k)} \Delta \boldsymbol{x}_{\mathrm{p}}^{(k+1)}\right] \\
=\ &-\left(\boldsymbol{x}_{\mathrm{p}} - \boldsymbol{W}_x \boldsymbol{n}\right)^{(k)}, \qquad (31)
\end{aligned}$$

combined with (27), yields

$$\begin{aligned}
&\Delta \boldsymbol{x}_{\mathrm{p}}^{(k+1)} + \boldsymbol{W}_x \left(\frac{\partial \boldsymbol{\theta}}{\partial \boldsymbol{u}_{\mathrm{p}}}\right)^{(k)} \Delta t\ \Delta \boldsymbol{u}_{\mathrm{p}}^{(k+1)} \\
=\ &-\left(\boldsymbol{x}_{\mathrm{p}} - \boldsymbol{W}_x \boldsymbol{n}\right)^{(k)} - \boldsymbol{W}_x \left(\Delta \boldsymbol{n} + \boldsymbol{\theta} \Delta t\right)^{(k)}. \qquad (32)
\end{aligned}$$

Equations (30) and (32) are N_{c} equations written in the form of a Newton-Raphson iterative scheme, and can be solved with respect to the primary variables $\boldsymbol{u}_{\mathrm{p}}$. We note that, if the volume/isochoric balance residuals vanish, the scheme corresponds to a weighted mass balance approach, i.e., a weighting of (27) by $\left(\partial \boldsymbol{V}/\partial \boldsymbol{n}\right)_p$ and $\boldsymbol{W}_x$.

3.3.1. *IMPSAT scheme*

As an alternative to (30) and (32), we may use an IMPSAT scheme, in which the interblock flow terms $\boldsymbol{f}$ in $\boldsymbol{\theta} = \boldsymbol{f} - \boldsymbol{q}$ are treated explicitly with respect to the isochoric variables $\boldsymbol{x}_{\mathrm{p}}$. This means that the derivatives of interblock flow terms with respect to $\boldsymbol{x}_{\mathrm{p}}$ vanish. Consequently, (30) reduces to

$$\begin{aligned}
&\left[\left(\frac{\partial \boldsymbol{V}_{\mathrm{p}}}{\partial p}\right)^{(k)} - \left(\frac{\partial \boldsymbol{V}}{\partial p}\right)_{\boldsymbol{n}}^{(k)}\right] \Delta p^{(k+1)} + \left(\frac{\partial \boldsymbol{V}_{\mathrm{p}}}{\partial \boldsymbol{S}_{\mathrm{p}}}\right)^{(k)} \Delta \boldsymbol{S}_{\mathrm{p}}^{(k+1)} \\
+\ &\left(\frac{\partial \boldsymbol{V}}{\partial \boldsymbol{n}}\right)_p^{(k)} \left[\left(\frac{\partial \boldsymbol{\theta}}{\partial p}\right)^{(k)} \Delta p^{(k+1)} + \left(\frac{\partial \boldsymbol{\theta}}{\partial \boldsymbol{S}_{\mathrm{p}}}\right)^{(k)} \Delta \boldsymbol{S}_{\mathrm{p}}^{(k+1)}\right] \Delta t \\
-\ &\left(\frac{\partial \boldsymbol{V}}{\partial \boldsymbol{n}}\right)_p^{(k)} \left(\frac{\partial \boldsymbol{q}}{\partial \boldsymbol{x}_{\mathrm{p}}}\right)^{(k)} \Delta t\ \Delta \boldsymbol{x}_{\mathrm{p}}^{(k+1)} \\
=\ &-\left(\boldsymbol{V}_{\mathrm{p}} - \boldsymbol{V}\right)^{(k)} - \left(\frac{\partial \boldsymbol{V}}{\partial \boldsymbol{n}}\right)_p^{(k)} \left(\Delta \boldsymbol{n} + \boldsymbol{\theta} \Delta t\right)^{(k)}. \qquad (33)
\end{aligned}$$

For all gridblocks that do not contain fully implicit and variable source terms, $\partial \boldsymbol{q}/\partial \boldsymbol{x}_{\mathrm{p}}$ vanishes. Consequently, the equations (33) are pressure and saturation equations, decoupled from the rest of the system. Actually, (33) identifies the black-oil part of the compositional system.

Furthermore, the equations (32) can be written

$$\begin{aligned} & \Delta \boldsymbol{x}_{\mathrm{p}}^{(k+1)} - \boldsymbol{W}_x \left(\frac{\partial \boldsymbol{q}}{\partial \boldsymbol{x}_{\mathrm{p}}} \right)^{(k)} \Delta t \, \Delta \boldsymbol{x}_{\mathrm{p}}^{(k+1)} \\ = & -\left(\boldsymbol{x}_{\mathrm{p}} - \boldsymbol{W}_x \boldsymbol{n} \right)^{(k)} - \boldsymbol{W}_x \left(\Delta \boldsymbol{n} + \boldsymbol{\theta} \Delta t \right)^{(k)} \\ & -\boldsymbol{W}_x \left[\left(\frac{\partial \boldsymbol{\theta}}{\partial p} \right)^{(k)} \Delta p^{(k+1)} + \left(\frac{\partial \boldsymbol{\theta}}{\partial \boldsymbol{S}_{\mathrm{p}}} \right)^{(k)} \Delta \boldsymbol{S}_{\mathrm{p}}^{(k+1)} \right] \Delta t. \end{aligned} \tag{34}$$

Here, $\Delta p^{(k+1)}$ and $\Delta \boldsymbol{S}_{\mathrm{p}}^{(k+1)}$ can be determined in advance by (33) in gridblocks that do not contain fully implicit and variable source terms. Consequently, (34) can be solved one gridblock at a time (explicitly). Elsewhere, (33) and (34) must be solved simultaneously.

3.4. Choice of secondary equations

For the presented iterative scheme to produce non-trivial changes of the primary variables, all of the requirements (8), (12) and (13) cannot be fulfilled at every iteration level, i.e., we cannot have both exact mass balance and exact volume balance. However, as mentioned, N_{c} of the conservation requirements can be included among the secondary equations, and thus be fulfilled at every iteration level.

3.4.1. *Exact volume balance*

The volume/isochoric balance set of secondary equations is

$$\begin{aligned} \boldsymbol{V}_{\mathrm{p}} \left(\boldsymbol{u}_{\mathrm{p}}^{(k)} \right) - \boldsymbol{V} \left(p^{(k)}, \boldsymbol{u}_{\mathrm{s}}^{(k)} \right) &= \boldsymbol{0}, \\ \boldsymbol{x}_{\mathrm{p}}^{(k)} - \boldsymbol{W}_x \boldsymbol{n} \left(\boldsymbol{u}_{\mathrm{s}}^{(k)} \right) &= \boldsymbol{0}, \\ \boldsymbol{f}^o \left(p^{(k)}, \boldsymbol{u}_{\mathrm{s}}^{(k)} \right) - \boldsymbol{f}^g \left(p^{(k)}, \boldsymbol{u}_{\mathrm{s}}^{(k)} \right) &= \boldsymbol{0}, \end{aligned} \tag{35}$$

where variables placed in parentheses indicate assumed dependencies. Equations (35) can be solved with respect to the secondary variables $\boldsymbol{u}_{\mathrm{s}}$ by a Newton-Raphson scheme, with the excellent initial estimate

$$\boldsymbol{u}_{\mathrm{s}}^{(k,0)} = \boldsymbol{u}_{\mathrm{s}}^{(k-1)} + \left(\frac{d\boldsymbol{u}_{\mathrm{s}}}{d\boldsymbol{u}_{\mathrm{p}}} \right)^{(k-1)} \Delta \boldsymbol{u}_{\mathrm{p}}^{(k)}. \tag{36}$$

Here, $d\boldsymbol{u}_{\mathrm{s}}/d\boldsymbol{u}_{\mathrm{p}}$ are total derivatives. The fulfilment of (35) at level $k-1$ ensures that total derivatives can be determined, see appendix B.2. We note that, due to (36), only a few iteration steps are required.

By solving (35), we obtain volume balance and isochoric balance at every iteration level, so that the right hand sides of (30) and (32) only

contain mass balance discrepancies. The iteration is used to reduce the mass balance discrepancies below some tolerance.

Actually, the volume balance can be made exact, by calculating

$$V^j = \frac{n^j}{\xi^j\left(p, \boldsymbol{u}_\mathrm{s}\right)} \tag{37}$$

using

$$n^j = \xi^j\left(p, \boldsymbol{u}_\mathrm{s}\right) V_\mathrm{p} S^j, \tag{38}$$

instead of $n^j = n^j\left(\boldsymbol{u}_\mathrm{s}\right)$. Here, ξ^j is the molar density of phase j, while n^j is the total mole number of phase j.

3.4.2. *Exact mass balance*
The mass balance set of secondary equations is

$$\begin{aligned} \boldsymbol{n}\left(\boldsymbol{u}_\mathrm{s}^{(k)}\right) - \boldsymbol{n}^{n-1} + \boldsymbol{\theta}\left(\boldsymbol{u}_\mathrm{p}^{(k)}\right)\Delta t &= \boldsymbol{0}, \\ \boldsymbol{f}^o\left(p^{(k)}, \boldsymbol{u}_\mathrm{s}^{(k)}\right) - \boldsymbol{f}^g\left(p^{(k)}, \boldsymbol{u}_\mathrm{s}^{(k)}\right) &= \boldsymbol{0}. \end{aligned} \tag{39}$$

These equations may also be solved with respect to $\boldsymbol{u}_\mathrm{s}$. Here, the mass balance can be made exact, by first determining $\boldsymbol{n}^{(k)}$ directly from the mass balance requirement. We then solve for the remaining parts $\overline{\boldsymbol{u}}_\mathrm{s}$ of $\boldsymbol{u}_\mathrm{s}$, for instance the gas phase mole numbers, using the initial estimate

$$\overline{\boldsymbol{u}}_\mathrm{s}^{(k,0)} = \overline{\boldsymbol{u}}_\mathrm{s}^{(k-1)} + \left(\frac{\partial \overline{\boldsymbol{u}}_\mathrm{s}}{\partial \boldsymbol{n}}\right)_p^{(k-1)} \Delta \boldsymbol{n}^{(k)}. \tag{40}$$

However, the treatment of $\boldsymbol{\theta}$ as an explicit function of $\boldsymbol{u}_\mathrm{p}$, and not also as a function of $\boldsymbol{u}_\mathrm{s}$, and the calculation of total derivatives of $\boldsymbol{\theta}$ with respect to $\boldsymbol{u}_\mathrm{p}$ in the iterative scheme, requires some explanation.

Due to the interblock flow terms, $\boldsymbol{\theta}$ depends on variables of several gridblocks. Consequently, if a spatial dependence of $\boldsymbol{u}_\mathrm{s}$ is considered in (39), the size of the corresponding linearized system will be unsuitable. In addition, the spatial dependencies make it inconvenient to calculate total derivatives from the N_s relations (39), see appendix B.2.

To get around these problems, we regard the primary variables $\boldsymbol{u}_\mathrm{p}$ to always be volume/isochoric balance consistent in themselves. This is plausible, since the volume/isochoric balance requirements (12) and (13) can be interpreted as definitions of saturations and isochoric variables. Consequently, having determined the primary variables at some iteration level, we proceed by solving (35) with respect to the secondary variables $\boldsymbol{u}_\mathrm{s}$, and use this solution to update $\boldsymbol{\theta}$ and the (total) derivatives of $\boldsymbol{\theta}$. This defines $\boldsymbol{\theta}$ as a function of $\boldsymbol{u}_\mathrm{p}$ only. In the exact mass balance approach we subsequently solve (39) with respect to $\boldsymbol{u}_\mathrm{s}$, but $\boldsymbol{\theta}$ and the derivatives of $\boldsymbol{\theta}$ are not updated.

By solving (39), we obtain mass balance at every iteration level, so that the right hand sides of (30) and (32) only contain volume balance and isochoric balance discrepancies, respectively. The iteration is used to reduce the volume/isochoric discrepancies below some tolerance.

We note that the exact mass balance approach is somewhat similar to the approach of Watts, [3]. However, our approach includes isochoric variables and equations, and is therefore more general. In addition, we use an iterative scheme, while Watts only uses a single iteration. The iteration improves the quality of the solution.

Due to the solution of both (35) and (39) at every iteration level, the presented exact mass balance approach is more costly per iteration step than the presented exact volume balance approach. However, Coats et al., [5], report that their exact mass balance approach has better convergence properties than the exact volume balance approach of Coats, [2]. Increased costs per iteration step could thus possibly be compensated by a reduced number of iteration steps.

We must use numerical tests to investigate the performance of the two presented approaches. However, in order to compare our results to those reported by Coats et al., [5], we first compare our formulation to that of Coats, [2], and to that of Coats et al., [5].

4. Comparisons to the Approaches of Coats and Coats et al.

In the following, the presented exact volume balance approach is compared to the approach of Coats, [2], while the presented exact mass balance approach is compared to the approach of Coats et al., [5].

4.1. The approach of Coats (1980)

Coats, [2], includes hydrocarbon phase mole fractions among the primary and secondary variables, instead of isochoric variables and phase mole numbers. The isochoric balance (13) is therefore not required. In addition, a different framework is used to set up the iterative scheme, see Appendix C. Coats' scheme is a combination of the linearized mass balance requirement (8) and the linearized fugacity equalities (26). The linearization is in terms of both primary and secondary variables, implying that total derivatives are not calculated.

Instead of solving the fugacity equalities at each iteration level, Coats' iterative scheme is used to reduce both mass balance and phase equilibrium discrepancies. This is in contrast with our approach. We solve the secondary equations at every iteration level, so that we are

able to calculate precise volume derivatives and total derivatives. Admittedly, the phase equilibrium calculations increase the computational costs on a per-iteration basis, but they also exclude thermodynamic difficulties from the Jacobian. The latter may be advantageous in challenging thermodynamic cases.

In the fully implicit case, Coats uses the linearized mass balance scheme without reformulation. In non-fully implicit cases, Gaussian elimination of the Jacobian is used to form implicit equations. In [10], Coats states that the pressure equation is unique, and shows that the Gaussian elimination is equivalent to a weighting by the total partial volumes. However, no equations of the form (32) are derived. In other words, one must choose which mass balance equation(s) to replace.

We always reformulate all of the mass balance equations. For the exact volume/isochoric balance approach, the reformulation is equivalent to a preconditioning of the linearized mass balance equations by partial volumes and the matrix $\boldsymbol{W}_x$. The use of complementary equations and variables leads to a system that is better conditioned.

4.2. The approach of Coats et al. (1998)

Coats et al., [5], use the same variable set as Coats, [2], and the same framework, but include the requirement that the saturations should sum to unity as an extra secondary equation. Having determined the primary variables, Coats et al. obtain exact mass balance by solving a system similar to (39) with respect to the phase mole numbers. The solution of these equations yields a set of saturations that do not sum to unity. However, being a secondary residual, the volume discrepancy is taken care of by the iterative scheme, see appendix C.

An exact mass balance approach requires that the term $\boldsymbol{\theta}$ is fixed when (39) is solved. Coats et al. update $\boldsymbol{\theta}$ as a function of the primary and secondary variables provided by the iterative scheme. Here, phase equilibrium residuals appear. Consequently, $\boldsymbol{\theta}$ does not necessarily correspond to a phase equilibrium. However, by the subsequent solution of (39), all other terms correspond to a phase equilibrium.

In our exact mass balance approach, we solve the fugacity equalities twice, so that all terms are always in accordance with a chemical equilibrium. This is more costly on a per-iteration basis, but our approach excludes phase equilibrium problems from the iteration, thus improving the robustness of the formulation.

In addition, we note that the approach of Coats et al., [5], like the approach of Coats, [2], does not involve a general reformulation (preconditioning) of the system.

5. Numerical Comparison of the Exact Mass Balance Approach To the Exact Volume Balance Approach

In the following, we compare the numerical properties of the presented exact mass balance approach, referred to as EMAB, to those of the presented exact volume balance approach, referred to as EVOB. The main objective is to investigate whether exact mass balance leads to better convergence properties than exact volume balance, as suggested by Coats et al., [5], and, if so, whether the computational costs of EMAB may be less than those of EVOB. The latter is not obvious, since the computational costs per iteration step are larger for EMAB.

The comparison of EMAB to EVOB is based on two numerical test examples, for which we study convergence, precision, computational costs and the effect of relaxed convergence criteria.

5.1. Compared properties

5.1.1. *Convergence and precision*

We monitor convergence by the normalized primary solution changes,

$$dp^{(k)} < \epsilon_{dp}, \quad dp^{(k)} = \frac{N}{\sum p^{(k)}} \max \left| \Delta p^{(k)} \right|, \tag{41}$$

$$dS^{(k)} = \left\| \delta \boldsymbol{S}_{\mathrm{p}}^{(k)} \right\|_{\infty} < \epsilon_{dS}, \quad \delta \boldsymbol{S}_{\mathrm{p}}^{(k)} = \max \left| \Delta \boldsymbol{S}_{\mathrm{p}}^{(k)} \right|, \tag{42}$$

$$dx^{(k)} = \left\| \delta \boldsymbol{x}_{\mathrm{p}}^{(k)} \right\|_{\infty} < \epsilon_{dx}, \quad \delta \boldsymbol{x}_{\mathrm{p}}^{(k)} = \max \left| \left(\frac{\Delta \boldsymbol{x}_{\mathrm{p}}^{(k)}}{\boldsymbol{x}_{\mathrm{p}}^{(k)}} \right) \right|, \tag{43}$$

and by the normalized residuals

$$r_{\mathrm{c}}^{(k)} = \left\| \boldsymbol{r}_{c}^{(k)} \right\|_{\infty} < \epsilon_{c}, \qquad \boldsymbol{r}_{c}^{(k)} = \max \left| \left(\frac{\Delta \boldsymbol{n} + \boldsymbol{\theta} \Delta t}{\boldsymbol{n}} \right)^{(k)} \right|, \tag{44}$$

$$r_{V}^{(k)} = \left\| \boldsymbol{r}_{V}^{(k)} \right\|_{\infty} < \epsilon_{V}, \qquad \boldsymbol{r}_{V}^{(k)} = \max \left| \left(\frac{\boldsymbol{V}_{\mathrm{p}} - \boldsymbol{V}}{\phi V_{\mathrm{b}}} \right)^{(k)} \right|, \tag{45}$$

$$r_{x}^{(k)} = \left\| \boldsymbol{r}_{x}^{(k)} \right\|_{\infty} < \epsilon_{x}, \qquad \boldsymbol{r}_{x}^{(k)} = \max \left| \left(\frac{\boldsymbol{x}_{\mathrm{p}} - \boldsymbol{W}_{x} \boldsymbol{n}}{\boldsymbol{x}_{\mathrm{p}}} \right)^{(k)} \right|, \tag{46}$$

$$r_{f}^{(k)} = \left\| \boldsymbol{r}_{f}^{(k)} \right\|_{\infty} < \epsilon_{f}, \qquad \boldsymbol{r}_{f}^{(k)} = \max \left| \left(\frac{\boldsymbol{f}^{o} - \boldsymbol{f}^{g}}{\boldsymbol{f}^{g}} \right)^{(k)} \right|. \tag{47}$$

Here, N denotes the number of gridblocks, $\sum$ and max are taken over all gridblocks, and fractions of vectors are to be interpreted as fractions of the vector components.

The primary solution changes appear in the iterative scheme used to determine the primary variables. Provided that the Jacobian is calculated correctly, quadratic convergence is expected as the solution of the equations is approached. Consequently, (41), (42) and (43) should decrease quadratically, regardless of the approach used.

The quantities (44), (45), (46) and (47) are normalizations of the primary and secondary equation residuals. The normalization of (44) implies that the mass balance of components appearing in small amounts is regarded to be relatively more important than the mass balance of components appearing in larger amounts. The same idea is reflected in (46) and (47). However, for the volume balance (45), we do not want to give a phase appearing in small amounts greater importance. We therefore use the pore volume for normalization.

We note that, with EVOB, (45) is exact, (46) and (47) are below their convergence limits at every iteration level, while (44) is decreased during the iteration. With EMAB, (44) is exact, (47) is below its convergence limit at every iteration level, while (45) and (46) are decreased during the iteration. The precision of EVOB and EMAB is associated with the limits below which the residuals can be reduced.

5.1.2. *Computational costs*

We let the average time spent on each nonlinear iteration step for EVOB and EMAB be denoted α_{EVOB} and α_{EMAB}, respectively. The average is over each timestep, and we have argued that $\alpha_{\mathrm{EVOB}} < \alpha_{\mathrm{EMAB}}$. In addition, we let the number of nonlinear iteration steps per timestep for EVOB and EMAB be denoted β_{EVOB} and β_{EMAB}, respectively. According to Coats et al., [5], we could expect that $\beta_{\mathrm{EVOB}} > \beta_{\mathrm{EMAB}}$. Consequently, if

$$\alpha_{\mathrm{EVOB}}\,\beta_{\mathrm{EVOB}} > \alpha_{\mathrm{EMAB}}\,\beta_{\mathrm{EMAB}}, \tag{48}$$

which is equivalent to

$$\kappa_{\mathrm{EVOB}} = \frac{\beta_{\mathrm{EVOB}}}{\beta_{\mathrm{EMAB}}} > \frac{\alpha_{\mathrm{EMAB}}}{\alpha_{\mathrm{EVOB}}} = \kappa_{\mathrm{EMAB}}, \tag{49}$$

the total costs of EMAB for a timestep are less than the total costs of EVOB. However, if the inequality is turned the other way, EVOB is the less costly approach. We compare the computational costs of EMAB versus EVOB by monitoring κ_{EVOB} and κ_{EMAB} for each timestep.

5.2. Test cases

We use two different test cases. The first case is similar to the Third SPE Comparative Solution Project, [12], while the second is similar to the Fifth SPE Comparative Solution Project, [13].

5.2.1. *Case 1: Third SPE Comparative Solution Project*

Case 1 includes 9 hydrocarbon components and water, and a grid of dimensions $9 \times 9 \times 4$. The description of components, rock and grid properties is given in [12], where we use the fluid characterisation data provided for the project by Arco Oil and Gas Company. However, we neglect capillary pressure and water and rock compressibility. In addition, we use analytical relative permeability relations,

$$k_r^o = \left(\frac{S^o}{1 - S_{co}^w}\right)^{2.75}, \tag{50}$$

$$k_r^g = \left(\frac{S^g}{1 - S_{co}^w}\right)^{1.9}, \tag{51}$$

$$k_r^w = \left(\frac{S^w - S_{co}^w}{1 - S_{co}^w}\right)^{2.25}, \tag{52}$$

where k_r^j is the relative permeability of phase j. The connate water saturation is set to $S_{co}^w = 0.16$.

In [12], gas cycling, with rates specified for both injector and producer, is used. We use another scenario. A constant rate of 0.25 std m^3/s of methane is injected in gridblock (1,1,1) and a fixed bottom hole pressure producer (232.76 bars) in located in gridblock (9,9,4).

The initial conditions prescribed in [12] correspond to a rich retrograde gas condensate reservoir. The pressure at datum depth is 244.76 bars (3550 psia), the temperature is 366.48 K (200 °F) and only gas and connate water are present initially. However, from the start of the simulation, oil appears in the reservoir.

As a precise capturing of volumes is important when phases reappear/disappear, EVOB is more robust than EMAB in such cases. Consequently, a proper comparison cannot be done with the original initial conditions. We therefore let the state immediately after the oil phase reappearance period constitute the initial conditions for Case 1.

5.2.2. *Case 2: Fifth SPE Comparative Solution Project*

Case 2 includes 6 hydrocarbon components and water, and a grid of dimensions $7 \times 7 \times 3$. The description of component, rock and grid properties is given in [13], but we neglect capillary pressures and rock

and water compressibilities. In addition, we use analytical relative permeability relations,

$$k_r^o = 0.8 \left(\frac{S^o}{1 - S_{co}^w} \right)^{2.75}, \tag{53}$$

$$k_r^g = 0.74 \left(\frac{S^g}{1 - S_{co}^w} \right)^{1.9}, \tag{54}$$

$$k_r^w = \left(\frac{S^w - S_{co}^w}{1 - S_{co}^w} \right)^{2.25}. \tag{55}$$

where the connate water saturation is set to $S_{co}^w = 0.2$.

The initial conditions prescribed in [13], with a datum pressure of 275.79 bars (4000 psia) and a temperature of 344.26 K (160 °F) correspond to a reservoir of connate water and undersaturated oil.

The fifth SPE Comparative Solution Project describes a water-alternating-gas (WAG) injection cycle. We use another scenario. A constant gas rate of 3.933 std m^3/s (12000 Mscf/day) with composition specified in [13] is injected into gridblock (1,1,1) and a fixed bottom hole pressure producer (265.79 bars) is located in gridblock (7,7,3).

We choose Case 2 so that oil remains undersaturated throughout the simulation run. Consequently, there is no phase reappearance or disappearance, and the fugacity equalities are redundant.

5.2.3. *Test scenario*

For both cases, we use a simulation run of 30 timesteps, governed by

$$\Delta t^{n+1} = \min \left\{ \Delta t^n \min_u \left[\frac{(1+\lambda)\Delta u^n}{\Delta u^* + \lambda \Delta u^n} \right], 30 \right\} \text{ days}, \tag{56}$$

where Δt^{n+1} is the next timestep, Δt^n is the previous timestep, Δu^n is the change in the variable u over the previous timestep, Δu^* is the target variable change during the next timestep and λ is a tuning factor. The formula is due to Aziz and Settari, [14]. We use $\lambda = 0.5$, $\Delta p^* = 15.0$ bars and $\Delta S^{j,*} = 0.1$. The initial timestep is 1 day, and the simulator is run in fully implicit mode.

Each case is run several times. The first run is with very strict convergence criteria, and is used to investigate the convergence behaviour, including the ultimate limits below which the residuals can be reduced.

Subsequent runs are based on relaxed convergence criteria. We here study computational costs and discrepancies of pressure, saturations and normalized mole numbers from a reference solution obtained with strict convergence criteria.

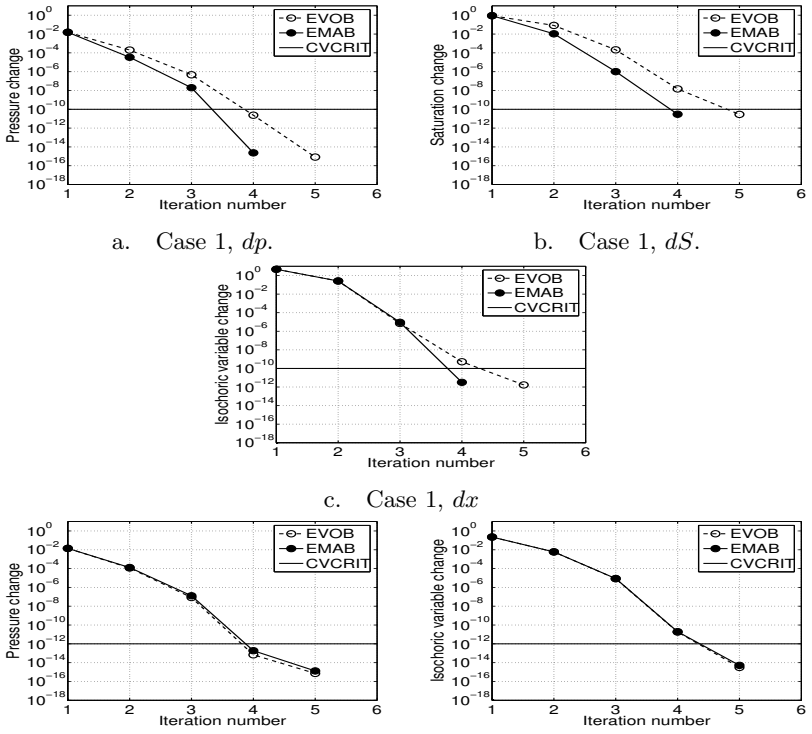

a. Case 1, *dp*. b. Case 1, *dS*.

c. Case 1, *dx*

d. Case 2, *dp*. e. Case 2, *dx*.

Figure 1. Typical behaviour of primary solution changes during a nonlinear iteration for Case 1 and Case 2. The notions *dp*, *dS* and *dx* refer to (41), (42) and (43), respectively. Convergence limits are also plotted. Note that there are no changes to the saturations (connate water and undersaturated oil) in Case 2.

5.3. Results

5.3.1. *Primary solution changes*

Figure 1 shows typical behaviour of the primary solution changes during a nonlinear iteration for Case 1 and Case 2. The notions *dp*, *dS* and *dx* refer to (41), (42) and (43), respectively. Here, we have used the same convergence limit for all solution changes and for all residuals (10^{-10} for Case 1 and 10^{-12} for Case 2). We note that the convergence limit can be set more strict for Case 2, as no saturation changes occur and no two-phase equilibrium has to be determined.

We observe a quadratic convergence behaviour for both EMAB and EVOB, indicating that the Newton-Raphson scheme is implemented properly. In Case 1, the convergence rate of EMAB is somewhat better, thus supporting the statements of Coats et al., [5]. However, for relaxed convergence criteria, the differences are less significant.

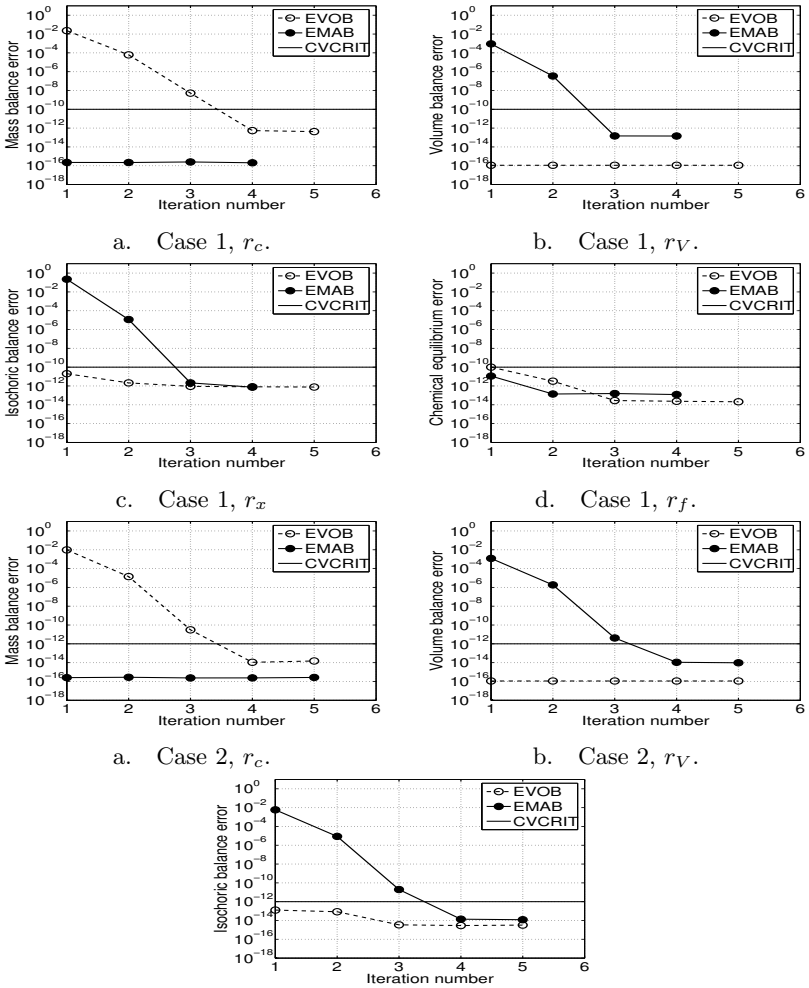

a. Case 1, r_c. b. Case 1, r_V.

c. Case 1, r_x d. Case 1, r_f.

a. Case 2, r_c. b. Case 2, r_V.

c. Case 2, r_x

Figure 2. Typical behaviour of residuals during a nonlinear iteration for Case 1 and Case 2. The notions r_c, r_V, r_x and r_f refer to (44), (45), (46) and (47), respectively, and the convergence limits are also plotted. Note that the fugacity equalities are redundant in Case 2.

5.3.2. *Precision*

Figure 2 shows typical behaviour of the equation residuals (44), (45), (46) and (47) during a nonlinear iteration for Case 1 and Case 2. We observe that the mass balance error r_{c} of EVOB and the volume balance error r_{v} of EMAB both flat out at about 10^{-12}, which is reasonably close to exact. The precision level obtained for the isochoric balance and the phase equilibrium is also similar for EVOB and EMAB.

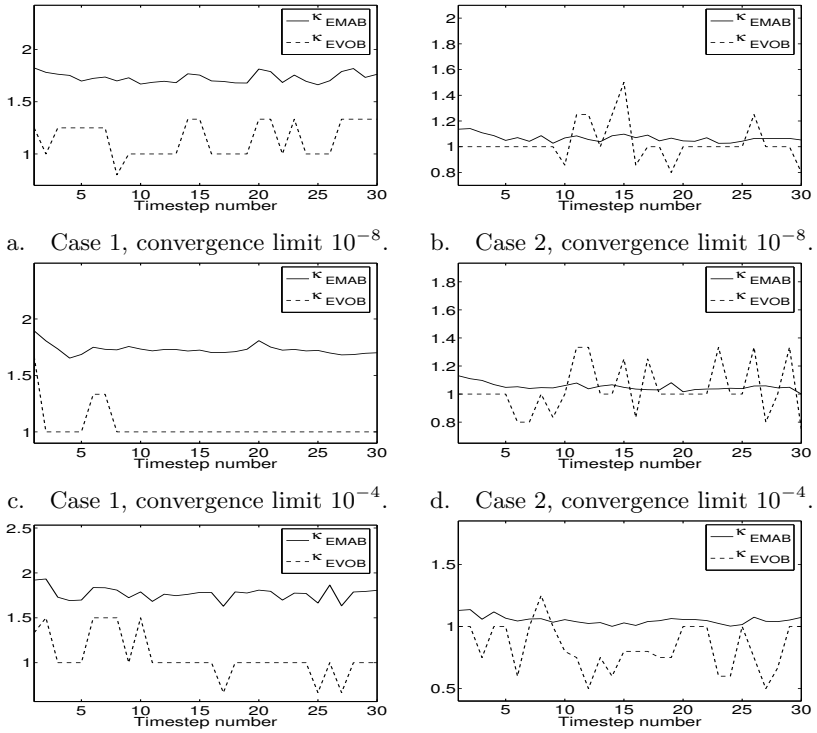

a. Case 1, convergence limit 10^{-8}. b. Case 2, convergence limit 10^{-8}.

c. Case 1, convergence limit 10^{-4}. d. Case 2, convergence limit 10^{-4}.

e. Case 1, convergence limit 10^{-2}. f. Case 2, convergence limit 10^{-2}.

Figure 3. Comparison of computational costs for Case 1 and Case 2, measured by κ_{EVOB} and κ_{EMAB} as defined by (49). Three different convergence limits are used for all solution changes and residuals: 10^{-8}, 10^{-4} and 10^{-2}.

5.3.3. *Computational costs*

Figure 3 shows a comparison of the computational costs of EVOB versus EMAB during the simulation runs, i.e., a comparison of κ_{EVOB} and κ_{EMAB}, as defined by (49). We recall that κ_{EVOB} is a measure of the possibly larger number of iteration steps required by EVOB, while κ_{EMAB} is a measure of the larger computational costs per iteration step for EMAB. Three different convergence limits used for all solution changes and residuals are tested: 10^{-8}, 10^{-4} and 10^{-2}.

For Case 1, EMAB is more costly throughout the run, regardless of the convergence limit. For Case 2, the redundant fugacity equalities lead to a smaller κ_{EMAB}, and κ_{EMAB} is both below and above κ_{EVOB} during the simulation run. For a convergence limit of 10^{-2}, the results are in favour of EVOB, but no strong conclusion can be made.

We note that relaxing the convergence limit only influences κ_{EVOB} and not κ_{EMAB}. This is what we should expect.

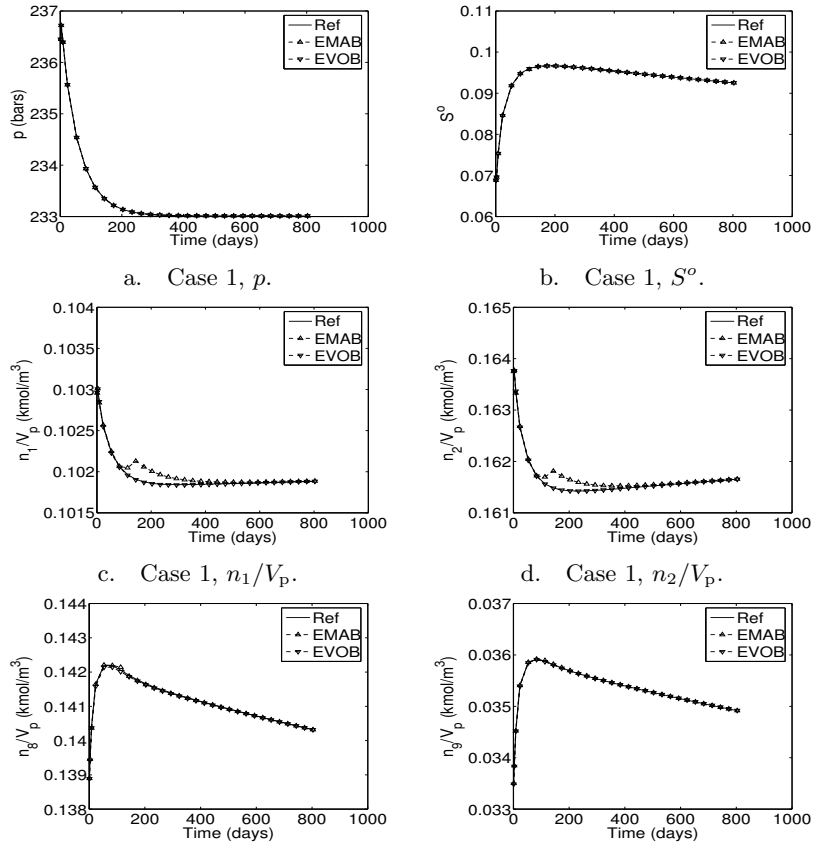

a. Case 1, p. b. Case 1, S^o.

c. Case 1, n_1/V_p. d. Case 1, n_2/V_p.

e. Case 1, n_8/V_p. f. Case 1, n_9/V_p.

Figure 4. Plots of the discrepancy between the solution obtained with a convergence limit of 10^{-2} and a reference solution (convergence limit 10^{-8}) of the production block for Case 1. The plots show the variations in pressure, oil saturation and pore volume normalized mole numbers of components 1, 2, 8 and 9 with time.

5.3.4. *Effect of relaxed convergence criteria*

When the convergence limit is relaxed, we expect discrepancies from a more precise solution. We use the solution for which the residuals are less than 10^{-8} as a reference solution, and compare it to the EMAB and EVOB solutions for which the residuals are required to be less than 10^{-2}. Figure 4 shows the comparison for Case 1, in terms of pressure, oil saturation and the pore volume normalized mole numbers of components 1, 2, 8 and 9 of the production block with time. For Case 2, the discrepancies are insignificant (do not show in plots).

We observe that the EMAB solution differs more from the reference solution than the EVOB solution does. However, this results clearly depends on the convergence criteria, which have implicitly been assumed

to be equivalent (same limit used for all residuals). Using different convergence limits for different residuals is not straight-forward, and is not considered here.

6. Conclusions and Further Work

A new compositional formulation which incorporates both an exact mass balance approach (EMAB) and an exact volume balance approach (EVOB) has been developed and tested. The form of the common iterative scheme clarifies the distinction between exact mass balance and exact volume balance, and motivates a comparison of the two approaches.

The comparison is seen in the light of the results reported by Coats et al., [5], i.e., that exact mass balance leads to better convergence properties than exact volume balance, and that exact mass balance therefore is preferable. However, our conclusions are in favour of exact volume balance. We have found some indications that EMAB may have a better convergence rate than EVOB, but this cannot compensate the fact that EMAB requires more computational effort per iteration step.

In addition, we have noted that EVOB is more robust than EMAB with respect to phase disappearance and reappearance. This is because a precise capturing of volumes is important in such cases.

The different conclusions are clearly implementation dependent. We note that Coats et al. compared an exact mass balance approach where the phase equilibrium is considered at every iteration level, [5], to an exact volume balance approach where phase equilibrium only is obtained as a result of the iteration, [2]. With our formulation, both approaches aim at phase equilibrium at every iteration level. This may be one of the reasons why we obtain results different from those reported by Coats et al., [5].

With respect to the ultimate precision that can be obtained, the two presented approaches are similar. EVOB can be used to obtain almost exact mass balance, while EMAB can be used to obtain almost exact volume balance. However, under relaxed convergence criteria, the discrepancies from a more precise solution seem to be larger for EMAB than for EVOB. This result is obtained by using the same convergence limit for all equation residuals. Using different limits for different residuals is not straight-forward, and is an interesting subject for further research.

Appendix

A. Mass Balance Inconsistency

To illustrate the inconsistency between the equations (21) and (22) and the conventional mass balance (8), we use $(p, \boldsymbol{S}_\mathrm{p}, \boldsymbol{x}_\mathrm{p}, V_\mathrm{b})$ as a complete set of parameters. Here, $\boldsymbol{S}_\mathrm{p}$ are $N_\mathrm{p} - 1$ primary saturations and a constant V_b is used to account for extensive quantities. In the following, subscripts on differentiation with respect to the variables $(p, \boldsymbol{S}_\mathrm{p}, \boldsymbol{x}_\mathrm{p})$ are omitted, while on differentiation with respect to $(p, \boldsymbol{n})$ they are not.

For simplicity, we assume that porosity is constant, so that $\boldsymbol{V}_\mathrm{p}$ is a linear function of the primary saturations $\boldsymbol{S}_\mathrm{p}$. Consequently, using $\boldsymbol{V}_\mathrm{p} = \boldsymbol{V}$ and assuming that $\boldsymbol{V} = \boldsymbol{V}(p, \boldsymbol{n})$, we obtain

$$\mathbf{0} = \frac{\partial \boldsymbol{V}_\mathrm{p}}{\partial p} = \frac{\partial \boldsymbol{V}}{\partial p} = \left(\frac{\partial \boldsymbol{V}}{\partial p}\right)_{\boldsymbol{n}} + \left(\frac{\partial \boldsymbol{V}}{\partial \boldsymbol{n}}\right)_{p} \frac{\partial \boldsymbol{n}}{\partial p}, \tag{57}$$

$$\Delta \boldsymbol{V}_\mathrm{p} = \frac{\partial \boldsymbol{V}_\mathrm{p}}{\partial \boldsymbol{S}_\mathrm{p}} \Delta \boldsymbol{S}_\mathrm{p} = \frac{\partial \boldsymbol{V}}{\partial \boldsymbol{S}_\mathrm{p}} \Delta \boldsymbol{S}_\mathrm{p} = \left(\frac{\partial \boldsymbol{V}}{\partial \boldsymbol{n}}\right)_{p} \frac{\partial \boldsymbol{n}}{\partial \boldsymbol{S}_\mathrm{p}} \Delta \boldsymbol{S}_\mathrm{p}, \tag{58}$$

$$\boldsymbol{O} = \frac{\partial \boldsymbol{V}_\mathrm{p}}{\partial \boldsymbol{x}_\mathrm{p}} = \frac{\partial \boldsymbol{V}}{\partial \boldsymbol{x}_\mathrm{p}} = \left(\frac{\partial \boldsymbol{V}}{\partial \boldsymbol{n}}\right)_{p} \frac{\partial \boldsymbol{n}}{\partial \boldsymbol{x}_\mathrm{p}}. \tag{59}$$

We also note that

$$\boldsymbol{W}_x \frac{\partial \boldsymbol{n}}{\partial p} = \frac{\partial \boldsymbol{x}_\mathrm{p}}{\partial p} = \mathbf{0}, \qquad \boldsymbol{W}_x \frac{\partial \boldsymbol{n}}{\partial \boldsymbol{S}_\mathrm{p}} = \frac{\partial \boldsymbol{x}_\mathrm{p}}{\partial \boldsymbol{S}_\mathrm{p}} = \boldsymbol{O}, \qquad \boldsymbol{W}_x \frac{\partial \boldsymbol{n}}{\partial \boldsymbol{x}_\mathrm{p}} = \frac{\partial \boldsymbol{x}_\mathrm{p}}{\partial \boldsymbol{x}_\mathrm{p}} = \boldsymbol{I}. \tag{60}$$

Here, $\boldsymbol{O}$ and $\boldsymbol{I}$ are zero and identity matrices of suitable dimensions.

Inserting these relations into (21) and (22), we obtain

$$\left(\frac{\partial \boldsymbol{V}}{\partial \boldsymbol{n}}\right)_{p} \left[\frac{\partial \boldsymbol{n}}{\partial p}\Delta p + \frac{\partial \boldsymbol{n}}{\partial \boldsymbol{S}_\mathrm{p}}\Delta \boldsymbol{S}_\mathrm{p} + \frac{\partial \boldsymbol{n}}{\partial \boldsymbol{x}_\mathrm{p}}\Delta \boldsymbol{x}_\mathrm{p} + \boldsymbol{\theta}\Delta t\right] = \mathbf{0}, \tag{61}$$

$$\boldsymbol{W}_x \left[\frac{\partial \boldsymbol{n}}{\partial p}\Delta p + \frac{\partial \boldsymbol{n}}{\partial \boldsymbol{S}_\mathrm{p}}\Delta \boldsymbol{S}_\mathrm{p} + \frac{\partial \boldsymbol{n}}{\partial \boldsymbol{x}_\mathrm{p}}\Delta \boldsymbol{x}_\mathrm{p} + \boldsymbol{\theta}\Delta t\right] = \mathbf{0}. \tag{62}$$

Consequently, equations (21) and (22) lead to

$$\frac{\partial \boldsymbol{n}}{\partial p}\Delta p + \frac{\partial \boldsymbol{n}}{\partial \boldsymbol{S}_\mathrm{p}}\Delta \boldsymbol{S}_\mathrm{p} + \frac{\partial \boldsymbol{n}}{\partial \boldsymbol{x}_\mathrm{p}}\Delta \boldsymbol{x}_\mathrm{p} + \boldsymbol{\theta}\Delta t = \mathbf{0}, \tag{63}$$

which is inconsistent with the conventional mass balance (8).

B. Calculation of Derivatives

B.1. Calculation of volume derivatives

The phase volumes $\boldsymbol{V}$ are thermodynamic properties, conventionally given in terms of pressure and the component mole numbers $\boldsymbol{n^j}$ of the phases, i.e.,

$$\boldsymbol{V} = \boldsymbol{V}\left(p, \boldsymbol{n^j}\right), \qquad V^j = V^j\left(p, \boldsymbol{n}^j\right). \tag{64}$$

Note that $\boldsymbol{n^j}$, containing the mole numbers of all phases, is different from $\boldsymbol{n}^j$, which only contains the mole numbers of phase j. The volume derivatives $\left(\partial \boldsymbol{V}/\partial p\right)_{\boldsymbol{n}}$ and $\left(\partial \boldsymbol{V}/\partial \boldsymbol{n}\right)_p$ are calculated with the additional assumption that

$$\boldsymbol{n^j} = \boldsymbol{n^j}\left(p, \boldsymbol{n}\right). \tag{65}$$

Consequently,

$$\left(\frac{\partial \boldsymbol{V}}{\partial p}\right)_{\boldsymbol{n}} = \left(\frac{\partial \boldsymbol{V}}{\partial p}\right)_{\boldsymbol{n^j}} + \left(\frac{\partial \boldsymbol{V}}{\partial \boldsymbol{n^j}}\right)_p \left(\frac{\partial \boldsymbol{n^j}}{\partial p}\right)_{\boldsymbol{n}}, \tag{66}$$

$$\left(\frac{\partial \boldsymbol{V}}{\partial \boldsymbol{n}}\right)_p = \left(\frac{\partial \boldsymbol{V}}{\partial \boldsymbol{n^j}}\right)_p \left(\frac{\partial \boldsymbol{n^j}}{\partial \boldsymbol{n}}\right)_p, \tag{67}$$

which require the calculation of derivatives of $\boldsymbol{n^j}$ with respect to $(p, \boldsymbol{n})$.

For the water phase and for the single hydrocarbon phase case, these derivatives are trivial, since $\boldsymbol{n^j} = \boldsymbol{n}$. In the case of two hydrocarbon phases, we differentiate through

$$\begin{bmatrix} \boldsymbol{f}^o\left(p, \boldsymbol{n}^o\right) - \boldsymbol{f}^g\left(p, \boldsymbol{n}^g\right) \\ \boldsymbol{n} - \sum_{j=o,g} \boldsymbol{n}^j \end{bmatrix} = \boldsymbol{0}, \tag{68}$$

with respect to $(p, \boldsymbol{n})$, assuming the relation (65). This leads to a set of linear systems of equations that can be solved with respect to the derivatives of $\boldsymbol{n^j}$ with respect to $(p, \boldsymbol{n})$.

We note that the fulfilment of the phase equilibria relations is essential for the calculation of the volume derivatives (66) and (67).

B.2. Calculation of total derivatives

For a variable or relation that can be written explicitly as a function of the primary variables $\boldsymbol{u}_\mathrm{p}$, differentiation with respect to $\boldsymbol{u}_\mathrm{p}$ is straightforward. However, for some variable or relation $h = h\left[\boldsymbol{u}_\mathrm{p}, \boldsymbol{u}_\mathrm{s}\left(\boldsymbol{u}_\mathrm{p}\right)\right]$ we must calculate the total derivative

$$\frac{dh}{d\boldsymbol{u}_\mathrm{p}} = \left(\frac{\partial h}{\partial \boldsymbol{u}_\mathrm{p}}\right)_{\boldsymbol{u}_\mathrm{s}} + \left(\frac{\partial h}{\partial \boldsymbol{u}_\mathrm{s}}\right)_{\boldsymbol{u}_\mathrm{p}} \frac{d\boldsymbol{u}_\mathrm{s}}{d\boldsymbol{u}_\mathrm{p}}. \tag{69}$$

Here, the calculation of $d\boldsymbol{u}_\mathrm{s}/d\boldsymbol{u}_\mathrm{p}$ requires that we have access to N_s fulfilled secondary relations $\boldsymbol{r}_\mathrm{s} = \boldsymbol{r}_\mathrm{s}\left(\boldsymbol{u}_\mathrm{p}, \boldsymbol{u}_\mathrm{s}\left(\boldsymbol{u}_\mathrm{p}\right)\right) = \boldsymbol{0}$, where N_s is the number of secondary variables $\boldsymbol{u}_\mathrm{s}$. Then,

$$\frac{d\boldsymbol{r}_\mathrm{s}}{d\boldsymbol{u}_\mathrm{p}} = \left(\frac{\partial \boldsymbol{r}_\mathrm{s}}{\partial \boldsymbol{u}_\mathrm{p}}\right)_{\boldsymbol{u}_\mathrm{s}} + \left(\frac{\partial \boldsymbol{r}_\mathrm{s}}{\partial \boldsymbol{u}_\mathrm{s}}\right)_{\boldsymbol{u}_\mathrm{p}} \frac{d\boldsymbol{u}_\mathrm{s}}{d\boldsymbol{u}_\mathrm{p}} = \boldsymbol{0}, \tag{70}$$

which leads to

$$\frac{d\boldsymbol{u}_\mathrm{s}}{d\boldsymbol{u}_\mathrm{p}} = -\left[\left(\frac{\partial \boldsymbol{r}_\mathrm{s}}{\partial \boldsymbol{u}_\mathrm{s}}\right)_{\boldsymbol{u}_\mathrm{p}}\right]^{-1} \left(\frac{\partial \boldsymbol{r}_\mathrm{s}}{\partial \boldsymbol{u}_\mathrm{p}}\right)_{\boldsymbol{u}_\mathrm{s}}. \tag{71}$$

We note that the fulfilment of N_s secondary relations is essential for the calculation of total derivatives.

C. The Framework of Coats

In the following, we present the framework proposed by Coats, [2], for deriving an iterative scheme to be solved for the primary variables $\boldsymbol{u}_\mathrm{p}$.

The N_c mass balance equations are referred to as the primary equations, and are written in the form

$$\boldsymbol{r}_\mathrm{p} = \boldsymbol{r}_\mathrm{p}\left(\boldsymbol{u}_\mathrm{p}, \boldsymbol{u}_\mathrm{s}\right) = \boldsymbol{0}. \tag{72}$$

The rest of the equations (constraint equations) are referred to as secondary equations, denoted

$$\boldsymbol{r}_\mathrm{s} = \boldsymbol{r}_\mathrm{s}\left(\boldsymbol{u}_\mathrm{p}, \boldsymbol{u}_\mathrm{s}\right) = \boldsymbol{0}. \tag{73}$$

Here, $\boldsymbol{u}_\mathrm{p}$ are the primary variables, and $\boldsymbol{u}_\mathrm{s}$ are the secondary variables. A linearization of the two sets of equations yields

$$\left(\frac{\partial \boldsymbol{r}_\mathrm{p}}{\partial \boldsymbol{u}_\mathrm{p}}\right)_{\boldsymbol{u}_\mathrm{s}}^{(k)} \Delta\boldsymbol{u}_\mathrm{p}^{(k+1)} + \left(\frac{\partial \boldsymbol{r}_\mathrm{p}}{\partial \boldsymbol{u}_\mathrm{s}}\right)_{\boldsymbol{u}_\mathrm{p}}^{(k)} \Delta\boldsymbol{u}_\mathrm{s}^{(k+1)} = -\boldsymbol{r}_\mathrm{p}^{(k)}, \tag{74}$$

$$\left(\frac{\partial \boldsymbol{r}_\mathrm{s}}{\partial \boldsymbol{u}_\mathrm{p}}\right)_{\boldsymbol{u}_\mathrm{s}}^{(k)} \Delta\boldsymbol{u}_\mathrm{p}^{(k+1)} + \left(\frac{\partial \boldsymbol{r}_\mathrm{s}}{\partial \boldsymbol{u}_\mathrm{s}}\right)_{\boldsymbol{u}_\mathrm{p}}^{(k)} \Delta\boldsymbol{u}_\mathrm{s}^{(k+1)} = -\boldsymbol{r}_\mathrm{s}^{(k)}. \tag{75}$$

From the latter, it is deduced that

$$\Delta\boldsymbol{u}_\mathrm{s}^{(k+1)} = -\left[\left(\frac{\partial \boldsymbol{r}_\mathrm{s}}{\partial \boldsymbol{u}_\mathrm{s}}\right)_{\boldsymbol{u}_\mathrm{p}}^{(k)}\right]^{-1} \left[\left(\frac{\partial \boldsymbol{r}_\mathrm{s}}{\partial \boldsymbol{u}_\mathrm{p}}\right)_{\boldsymbol{u}_\mathrm{s}}^{(k)} \Delta\boldsymbol{u}_\mathrm{p}^{(k+1)} + \boldsymbol{r}_\mathrm{s}^{(k)}\right], \tag{76}$$

which, when inserted into the former, yields

$$\left[\left(\frac{\partial \boldsymbol{r}_\mathrm{p}}{\partial \boldsymbol{u}_\mathrm{p}}\right)^{(k)}_{\boldsymbol{u}_\mathrm{s}} - \left(\frac{\partial \boldsymbol{r}_\mathrm{p}}{\partial \boldsymbol{u}_\mathrm{s}}\right)^{(k)}_{\boldsymbol{u}_\mathrm{p}} \left[\left(\frac{\partial \boldsymbol{r}_\mathrm{s}}{\partial \boldsymbol{u}_\mathrm{s}}\right)^{(k)}_{\boldsymbol{u}_\mathrm{p}}\right]^{-1} \left(\frac{\partial \boldsymbol{r}_\mathrm{s}}{\partial \boldsymbol{u}_\mathrm{p}}\right)^{(k)}_{\boldsymbol{u}_\mathrm{s}}\right] \Delta \boldsymbol{u}_\mathrm{p}^{(k+1)} = -\boldsymbol{r}_\mathrm{p}^{(k)} + \left(\frac{\partial \boldsymbol{r}_\mathrm{p}}{\partial \boldsymbol{u}_\mathrm{s}}\right)^{(k)}_{\boldsymbol{u}_\mathrm{p}} \left[\left(\frac{\partial \boldsymbol{r}_\mathrm{s}}{\partial \boldsymbol{u}_\mathrm{s}}\right)^{(k)}_{\boldsymbol{u}_\mathrm{p}}\right]^{-1} \boldsymbol{r}_\mathrm{s}^{(k)}. \quad (77)$$

Equations (77) can be used to determine the primary variables, and is accompanied by the update (76) of the secondary variables. Consequently, both $\boldsymbol{r}_\mathrm{p}$ and $\boldsymbol{r}_\mathrm{s}$ take part in the iteration.

References

[1] L. C. Young and R. E. Stephenson. A Generalized Compositional Approach for Reservoir Simulation. SPEJ, (1983) 727–42.

[2] K. H. Coats. An Equation of State Compositional Model. SPEJ, (1980), 363–76.

[3] J. W. Watts. A Compositional Formulation of the Pressure and Saturation Equations. SPE 12244, SPE Reservoir Engineering, (1986) 243–252.

[4] P. Quandalle and D. Savary. An Implicit in Pressure and Saturations Approach to Fully Compositional Simulation. SPE 18423, in: *Proc. of the 10th SPE Symposium on Reservoir Simulation*, Houston, TX, 1989, pp. 197–206.

[5] K. H. Coats, L. K. Thomas, and R. G. Pierson. Compositional and Black Oil Reservoir Simulation. SPE 50990, SPE Reservoir Evaluation and Engineering 1(4) (1998) 372–379.

[6] H. Cao. *Development of Techniques for General Purpose Simulators*. Ph.D. diss., Department of Petroleum Engineering, Stanford University, CA (2002).

[7] J. Haukås, I. Aavatsmark, M. Espedal, and E. Reiso. A Volume Balance Consistent Compositional IMPSAT Formulation With Relaxed Stability Constraints. Submitted to: Computational Geosciences 2005.

[8] G. Ács, S. Doleschall, and É. Farkas. General Purpose Compositional Model. SPEJ, (1985) 543–553.

[9] T. Wong, A. Firoozabadi and K. Aziz. The Relationship between the Volume Balance Method and the Newton-Raphson Method of Compositional Simulation. SPE 18424, in: *Proc. of the Tenth SPE Symposium on Reservoir Simulation*, Houston, TX, 1989.

[10] K. H. Coats. A Note on Impes and Some Impes-Based Simulation Models. SPE 49774, in: *Proc. of the 15th SPE Symposium on Reservoir Simulation*, Houston, TX, 1999, pp. 21–39.

[11] Geoquest, Schlumberger. *Eclipse 300 Technical Description 2002A*. www.sis.slb.com/content/software/simulation/eclipse_compositional.asp, 2002.

[12] D. E. Kenyon and G. A. Behie. Third SPE Comparative Solution Project: Gas Cycling of Retrograde Condensate Reservoirs. SPE 12278, in: *Proc. of the 7th SPE Symposium on Reservoir Simulation*, San Francisco, CA, 1983.

[13] J. E. Killough and C. A. Kossack. Fifth Comparative Solution Project: Evaluation of Miscible Flood Simulators. SPE 16000, in: *Proc. of the 9th SPE Symposium on Reservoir Simulation*, San Antonio, TX, 1987, pp. 55–73.

[14] K. Aziz and A. Settari. *Petroleum Reservoir Simulation.* (Applied Science Publishers, London, 1979).